

---

---

# **<sup>18</sup>F-FDG PET/MRI compared with clinical and serological markers for monitoring disease activity in patients with aortitis and chronic periaortitis**

---

I. Einspieler<sup>1,5</sup>, M. Henninger<sup>1</sup>, V. Mergen<sup>1</sup>, H. Wendorff<sup>2</sup>,  
B. Haller<sup>3</sup>, L.P. Beyer<sup>5</sup>, P. Moog<sup>4</sup>, K. Thürmel<sup>4</sup>

---

Departments of <sup>1</sup>Nuclear Medicine, <sup>2</sup>Vascular Surgery, <sup>3</sup>Medical Statistics and Epidemiology, <sup>4</sup>Nephrology and Rheumatology, Klinikum rechts der Isar, School of Medicine, Technical University of Munich, and <sup>5</sup>Department of Radiology, University Hospital Regensburg, Germany.

Ingo Einspieler, MD  
Martin Henninger, MD  
Victor Mergen, MD  
Heiko Wendorff, MD  
Bernhard Haller, PhD  
Lukas P. Beyer, MD  
Philipp Moog, MD\*  
Klaus Thürmel, MD\*

\*These authors share last authorship.

Please address correspondence to:

Ingo Einspieler,  
University Hospital Regensburg,  
Franz-Josef-Strauß-Allee 11,  
93053 Regensburg, Germany.  
E-mail: ingo.einspieler@ukr.de

Received on January 6, 2020; accepted in revised form on March 11, 2020.

*Clin Exp Rheumatol* 2020; 38 (Suppl. 124): S99-S106.

© Copyright CLINICAL AND EXPERIMENTAL RHEUMATOLOGY 2020.

**Key words:** aortitis, chronic periaortitis, magnetic resonance imaging, positron-emission tomography, vasculitis

Competing interests: none declared.

## **ABSTRACT**

**Objective.** We compared the diagnostic value of fully integrated <sup>18</sup>F-FDG PET/MRI to that of clinical and serological markers for monitoring disease activity in patients with aortitis/chronic periaortitis (A/CPA) during immunosuppressive therapy.

**Methods.** Patients positive for A/CPA at the initial and at least 2 consecutive PET/MRI studies were included for retrospective analysis. Imaging (qualitative and quantitative analysis), clinical, and serologic (C-reactive protein, erythrocyte sedimentation rate) assessments were determined at each visit, and their findings compared. Differences in various PET/MRI parameters, clinical symptoms, and serologic markers during therapy between first and second visits were tested for statistical significance. Spearman's rank correlation coefficient was calculated to relate imaging to serologic marker changes between the first 2 visits.

**Results.** Serial assessments were performed in 12 patients with A/CPA, over 34 visits. PET/MRI suggested active disease in 22/34 (64.7%) studies, whereas clinical assessment and serological analysis were positive in only 18/34 (52.9%) and 17/34 (50%) cases, respectively. Disease activity assessment differed between PET/MRI, and clinical and serological markers, in 8/34 (23.5%) and 9/34 (26.5%) cases, respectively. Imaging and serologic parameters ( $p < 0.009$ ) and clinical symptoms ( $p = 0.063$ ) predominantly improved at the second visit. Changes from the first to the second visit were not correlated between PET/MRI and serologic markers.

**Conclusion.** Fully integrated <sup>18</sup>F-FDG PET/MRI provides a comprehensive imaging approach with data on vascu-

lar/perivascular inflammation that is complementary to clinical and laboratory assessments. This highlights the potential value of imaging-based disease activity monitoring, which might have a crucial impact on clinical management in patients with A/CPA.

## **Introduction**

Aortitis and chronic periaortitis (A/CPA) are rare conditions, usually autoimmune-mediated and characterised by inflammation of the aortic wall or periaortic tissue. The former, encompassing giant cell arteritis (GCA) and Takayasu's arteritis (TAK), as the two main forms of large-vessel vasculitis (LVV), is secondary to a systemic granulomatous vasculitis that involves inflammatory cellular infiltrates of multinucleated giant cells, mononuclear cells, lymphocytes, and a high degree of vascularisation in its acute phase, while progressive fibrosis prevails in the chronic stage (1). In contrast, in chronic periaortitis, including idiopathic retroperitoneal fibrosis, perianeurysmal retroperitoneal fibrosis, and inflammatory abdominal aortic aneurysm, a mixture of fibrous tissue and inflammatory infiltrates, with predominantly mononuclear cell infiltrates within fibroblasts and collagen bundles, is found in highly vascular and oedematous tissue during the active inflammatory phase. In the late stages of this disease entity, histology shows pronounced sclerosis and scattered calcifications (2).

Chronic periaortitis is usually located at the abdominal aorta and the iliac arteries and its pathogenesis is considered to be secondary to a localised inflammatory reaction to atherosclerotic plaque antigens (3). However, recent observations have suggested that chronic periaortitis may arise as a pri-

mary LVV, with inflammation predominating in the adventitia of the aorta, similarly to that seen in GCA and TAK, which is typically localised to the abdominal aorta and its branches in some patients, and in others extends to other vascular segments (4-7).

Both aortitis and chronic periaortitis go through different phases of inflammatory activity, mostly in the form of flare-ups, with later degeneration into more or less active stages of fibrosis (8, 9). Distinguishing between florid and dormant A/CPA is crucial for guiding clinical management and allowing individualised treatment, as untreated inflammation can result in irreversible damage to the large arteries and immunosuppressive treatment for A/CPA carries potential life-threatening risks (10). Traditionally, disease activity is assessed by C-reactive protein (CRP) levels and erythrocyte sedimentation rate (ESR), along with clinical parameters, rather than by vascular imaging. However, acute-phase reactants are not specific, yielding false-negative and false-positive findings in 20%-40% of cases (6, 8, 11-13). In addition, CRP and ESR rapidly normalise after commencing treatment with novel interleukin-6 receptor alpha inhibitor therapeutic agents, which hampers the assessment of disease activity (14-16). Moreover, clinical features of A/CPA may be non-specific (*e.g.* headaches, back pain) or may potentially be related to prior vascular/perivascular damage, rather than to active inflammation (*e.g.* limb claudication, hydronephrosis).

These dilemmas have encouraged the increasing use of different imaging techniques for diagnosis, assessment of disease activity, and even therapy monitoring of A/CPA (8, 9, 17-20). To date, a few studies have evaluated the role of  $^{18}\text{F}$ -fluorodeoxyglucose positron-emission tomography ( $^{18}\text{F}$ -FDG PET), computed tomography (CT), and magnetic resonance imaging (MRI) for monitoring A/CPA in established cases (8, 9, 18, 21-24). Based on the currently available data, none of these different imaging methods is clearly preferred over another for monitoring disease activity in A/CPA. Thus, imaging is not recommended by the European League

Against Rheumatism (EULAR) for follow-up examinations to investigate potential ongoing inflammation in patients without clinically/serologically suspected flare, since its usefulness is not yet defined (25). There is, however, an unmet need to identify patients at risk of relapse and those with sub-clinical activity, by introducing novel diagnostic imaging techniques and by A/CPA-specific image acquisition protocols, respectively.

In the past decade,  $^{18}\text{F}$ -FDG PET/CT has emerged as a novel and powerful imaging modality in the evaluation of inflammatory disorders such as A/CPA. However, high radiation exposure, low soft tissue contrast and potential adverse effects of CT contrast media remain an issue. As opposed to that, non-invasive molecular hybrid imaging by means of fully integrated  $^{18}\text{F}$ -FDG PET/MRI allows precise combination of  $^{18}\text{F}$ -FDG PET and radiation free vascular MRI in a one-stop-shop procedure for simultaneous assessment of disease activity as well as possible late/chronic structural A/CPA complications, as shown by our group in preliminary studies (6, 26). Recently,  $^{18}\text{F}$ -FDG PET/MRI findings have been successfully correlated with clinical characteristics and outcome in patients with LVV in a small prospective trial by Laurent *et al.* (27). The authors conclude that  $^{18}\text{F}$ -FDG PET/MRI could facilitate the characterisation of disease activity, especially for challenging cases. In view of its presumable benefit in revealing different aspects and stages of the complex inflammatory process by providing multiparametric information, we hypothesised that whole-body  $^{18}\text{F}$ -FDG PET/MRI might provide additive diagnostic value in monitoring disease activity in patients with A/CPA undergoing immunosuppressive therapy, over that provided by established clinical and serological markers.

## Materials and methods

### Study population

Twelve patients positive for A/CPA at the initial and at least 2 consecutive PET/MRI studies were extracted from the institutions' database (June 2013 to January 2018) for retrospective analy-

sis. At baseline, patients underwent PET/MRI during the primary diagnostic evaluation ( $n=7$ ) or during follow-up in cases of relapse ( $n=5$ ). The second PET/MRI scan was performed to assess disease activity and disease progression/non-progression during immunosuppressive therapy, which was started or escalated after the first visit. Ten additional follow-up PET/MRI studies in 6 patients under/after immunosuppressive medication treatment were performed (*i.e.* a third PET/MRI scan in 6 cases, and a fourth PET/MRI scan in 4 cases), in two of those due to relapse at the third visit, whereas in the other ones imaging was applied to assess activity and progression/non-progression during follow-up. The local Ethics Committee approved the study, and we obtained written informed consent from all participants for the purpose of anonymised evaluation and publication of their data. Study population characteristics and immunosuppressive therapy details are summarised in Table I.

### PET/MRI acquisition

Imaging was performed on a Biograph mMR (Siemens Medical Solutions, Erlangen, Germany), which allows whole-body simultaneous acquisition of PET and 3-Tesla MRI data. A vascular-specific PET/MRI protocol, encompassing a coronal whole-body T2-weighted (T2w) short  $\tau$  inversion recovery (STIR) sequence with fat suppression, whole-body contrast-enhanced magnetic resonance angiography (CE-MRA) with continuous table movement, and axial T1w fat-suppressed three-dimensional (3D) volumetric interpolated breath-hold examination (VIBE) sequences pre- and post-contrast media administration, covering the trunk, was implemented (6, 26). The technical specifications of the PET/MRI scanner used are summarised in a performance evaluation paper (28). Patients fasted for at least 6 h before  $^{18}\text{F}$ -FDG injection. Blood glucose levels were below 150 mg/dl in all patients. On average, the PET/MRI scan was started with 8 bed positions, with a 2-4-minute acquisition time per bed position,  $121\pm 35$  min after injection of  $352\pm 76$  MBq  $^{18}\text{F}$ -FDG. A mean of  $25\pm 1$  ml Magnograft®

**Table I.** Epidemiological and therapy data.

Patient	Sex	Age at 1 <sup>st</sup> visit	Underlying disease of A/CPA	Prior Therapy	Medication at 1 <sup>st</sup> visit	Medication at 2 <sup>nd</sup> visit	Medication at 3 <sup>rd</sup> visit	Medication at 4 <sup>th</sup> visit
1*	F	58	IRF	-	-	GC (10 mg/day)	<u>GC</u> , <u>MMF</u>	GC (5 mg/day), <u>RTX</u> , <u>MMF</u>
2*	F	49	IRF	-	-	GC (8 mg/day)	MTX, <u>GC</u>	MTX
3	M	60	PRF	GC	-	MMF, <u>GC</u> , <u>RTX</u>	N/A	N/A
4	M	59	PRF	-	-	GC (10 mg/day), MTX	N/A	N/A
5	M	65	PRF	GC	-	MMF, <u>GC</u>	N/A	N/A
6*	F	59	GCA	-	-	GC (5 mg/day), MTX	<u>GC</u>	N/A
7*	M	68	GCA	GC	GC (20 mg/day)	MTX, <u>GC</u>	MTX, <u>GC</u>	<u>MTX</u>
8	M	73	GCA	-	-	MTX, <u>GC</u>	N/A	N/A
9	M	71	GCA	-	-	GC (5 mg/day), TOC	N/A	N/A
10	F	63	GCA	-	-	MTX, <u>GC</u>	N/A	N/A
11*	F	28	TAK	GC	-	<u>GC</u> , <u>LEF</u>	-	N/A
12*	F	29	TAK	GC, MTX, TOC	GC (1 mg/day)	GC (2.5 mg/day), TOC	<u>MTX</u> , <u>TOC</u>	-

The mean time interval between the first and second visit was 11.8 months (range: 2–24 months). In the subgroup of patients with more than 1 follow-up study (\*n = 6), the mean time interval between the first and third visit was 20.2 months (range: 11–33 months) and between the first and fourth visit was 28.8 months (range: 23–33 months).

M: male; F: female; A/CPA: aortitis/chronic periaortitis; IRF: idiopathic retroperitoneal fibrosis; PRF: perianeurysmal retroperitoneal fibrosis; GCA: giant cell arteritis; TAK: Takayasu’s arteritis; GC: glucocorticoids; MTX: methotrexate; TOC: tocilizumab; MMF: mycophenolate mofetil; RTX: rituximab; LEF: leflunomide; N/A: not applicable.

Underlined and italic terms indicate that immunosuppressive medication was given between the current and prior visit, but with discontinuation in-between.

was administered to acquire contrast-enhanced MRI data.

#### Imaging assessment

PET scans were evaluated by 2 experienced board-certified nuclear medicine physicians in consensus on a dedicated workstation and software (syngo MMWP and syngo TrueD, Siemens Medical Solutions). Readers were blinded to clinical, laboratory, and MRI findings, but unblinded to previous PET images. Disease activity was defined by global interpretation of each study based upon assessment of the following 15 vascular territories: brachiocephalic trunk, both subclavian arteries, both vertebral arteries, both common carotid arteries, ascending aorta, aortic arch, descending thoracic aorta, abdominal aorta, both iliac arteries, and both femoral arteries. For qualitative assessment, the degree of <sup>18</sup>F-FDG uptake relative to the liver was visually scored from 0 to 3 (Visual score, VS; 0 = no uptake; 1 = uptake present, but lower than liver uptake; 2 = uptake similar to liver uptake; 3 = higher than liver uptake), in accordance with recent recommendations (25, 29). To assess the qualitative burden of vascular/perivascular FDG uptake across multiple vessel regions, a modified version of a recently introduced global summary score (PET

vascular activity score, PETVAS, (23)) was calculated by adding the VS in the 15 territories (instead of 9 territories as applied by Grayson PC *et al.* (23)), with scores ranging from 0–45. For quantitative evaluation, the maximal standardised uptake value (SUV<sub>max</sub>) and the highest target to blood pool ratio (TBR) were evaluated in each patient (26).

MRI scans were assessed quantitatively and qualitatively by 2 experienced board-certified radiologists using an FDA-approved OsiriX DICOM viewer (OsiriX MD v.10.0.3), blinded to clinical, laboratory, and PET findings, but unblinded to previous MRI studies. Consensus between the readers was used considering all available sequences to determine whether each scan was consistent with active or inactive A/CPA. Images were evaluated for maximum thickening (MT) and increased contrast-enhancement (ICE) of the aortic wall/periaortic tissue in the axial plane, respectively. The presence of T2 STIR signal hyperintensity, as a proxy for oedema, was assessed at the aorta and its branches by comparing the mural/perimural signal intensity with myocardial intensity (18). In CE-MRA analysis, vessel narrowing/occlusion and aneurysms/ectasia were documented. Vascular territories that were not adequately visualised or were

sites of prior surgical intervention were excluded from analysis.

#### Clinical and laboratory assessment

At each visit, patients underwent detailed clinical and laboratory investigations. Clinically active disease was defined by the presence of at least 1 clinical symptom directly attributed to ongoing A/CPA by two rheumatologists in consensus with substantial experience in patients with inflammatory vascular/perivascular disorders. Abnormal acute-phase reactants (CRP, normal ≤0.5 mg/dl, and/or ESR, normal ≤20 mm) alone were not considered sufficient evidence of clinical disease activity. Clinical assessments were performed blinded to imaging data. A detailed history was obtained at each visit focusing on prior and current therapies, including glucocorticoids and other immunosuppressive medication (*e.g.* disease-modifying anti-rheumatic drugs and biologic agents). All patients received careful further workup to exclude infectious disease and other autoimmune or malignant disorders.

#### Statistical analysis

Wilcoxon’s signed-rank test and McNemar’s test were performed to evaluate differences in the distribution of continuous and categorical variables between

the first and second visit, respectively. Spearman's rank correlation coefficient was calculated to examine correlations between relative changes (*i.e.*  $V_{\text{visit2}} - V_{\text{visit1}}$ ) of imaging and laboratory inflammation markers of the first 2 visits. All statistical analyses were performed using MedCalc (v. 18.5). A significance level of  $\alpha=5\%$  was used for all statistical tests.

**Results**

*PET/MRI data*

At the first visit, 12/12 (100%) and 11/12 (91.7%) patients were classified as having active A/CPA according to PET and MRI analysis, respectively. The second examination demonstrated 4/12 (33.3%) PET-positive and 5/12 (41.7%) MRI-positive cases; thus, 5 cases were PET/MRI-positive in the combined analysis. Discrepant PET and MRI findings were found in 2 patients at the first 2 visits (*i.e.* 2/4 studies with discordant results). All but 1 (*i.e.* CE-MRA) assessed imaging parameters had significantly improved by the second visit (Table II, Fig. 1). This decrease was clinically relevant (*i.e.* normalisation) in 8/12 (66.7%), 7/11 (63.6%), and 8/11 (72.7%) patients, considering VS, ICE, and oedema imaging by T2w-MRI, respectively. CE-MRA showed progressive disease in 2 patients at the second visit, as follows: In 1 patient, a new ectasia of the suprarenal abdominal aorta was observed. In another patient with previously known long segmental stenosis of both vertebral arteries, a new occlusion of the right vertebral artery with consequent ischaemia in the cerebellum, occurred (Fig. 2). In these patients, the modified PETVAS score was substantial at the first visit (scores: 42-45) compared to 8 patients with low scores of 3-15 and another 2 patients with moderate-to-high scores of 32-43. At the third and fourth visit, 3/6 (50%) patients showed active A/CPA in 5/10 (50%) studies, as follows: in 1 patient, PET and MRI indicated typical findings for active CPA in 2 studies with additional findings suggestive of active LVV (Fig. 3). In another patient, MRI showed active CPA in 2 studies, whereas PET demonstrated a flare in 1 study (of note, this patient had already discordant PET and MRI results at

**Table II.** Differences in imaging, laboratory, and clinical parameters during therapy between the first 2 visits.

	Parameters	1 <sup>st</sup> Visit	2 <sup>nd</sup> Visit	p-value
<b>PET</b>	SUV <sub>max</sub> * <sup>1</sup>	8.5 (range: 3.2–13.4)	1.4 (range: 1–5.3)	0.001 <sup>1</sup>
	TBR* <sup>1</sup>	5.7 (range: 2.3–11.1)	1.3 (range: 0.9–4.2)	0.001 <sup>1</sup>
	VS* <sup>1</sup>	3 (range: 1–3)	1 (range: 0–3)	0.002 <sup>1</sup>
	mPETVAS	11 (range: 1–45)	5.5 (range: 0–24)	0.001 <sup>1</sup>
<b>MRI</b>	MT (mm)* <sup>2</sup>	6.9 (range: 3.7–43)	3.9 (range: 3–36)	0.001 <sup>1</sup>
	ICE	12/12 (100%)	4/12 (33.3%)	0.008 <sup>2</sup>
	Oedema	11/12 (91.7%)	3/12 (25%)	0.008 <sup>2</sup>
	LC by CE-MRA	8/12 (66.7%)	9/12 (75%)	1.000 <sup>2</sup>
<b>Serological assessment</b>	CRP	3.1 (range: 0.3–11.4)	0.5 (range: 0.1–1.8)	0.001 <sup>1</sup>
	ESR	44 (range: 1–125)	13 (range: 2–34)	0.006 <sup>1</sup>
<b>Clinical assessment</b>	Clinical symptoms	10/12 (83.3%)	5/12 (41.7%)	0.063 <sup>2</sup>

Data are expressed as median values (SUV<sub>max</sub>, TBR, VS, mPETVAS, MT, CRP, ESR) and number of patients (ICE, oedema, LC by MRA, clinical symptoms), respectively.

\*In each patient the highest value was used for statistical testing.

SUV<sub>max</sub>: maximum standardised uptake value; TBR: target to blood pool ratio; VS: visual score; mPETVAS: modified PET vascular activity score; MT: maximum thickening; ICE: increased contrast enhancement; LC: luminal changes (*i.e.* stenosis, occlusion, aneurysm, ectasia); CE-MRA: contrast-enhanced magnetic resonance angiography; CRP: C-reactive protein; ESR: erythrocyte sedimentation rate. 1: Wilcoxon signed rank test; 2: McNemar's test.

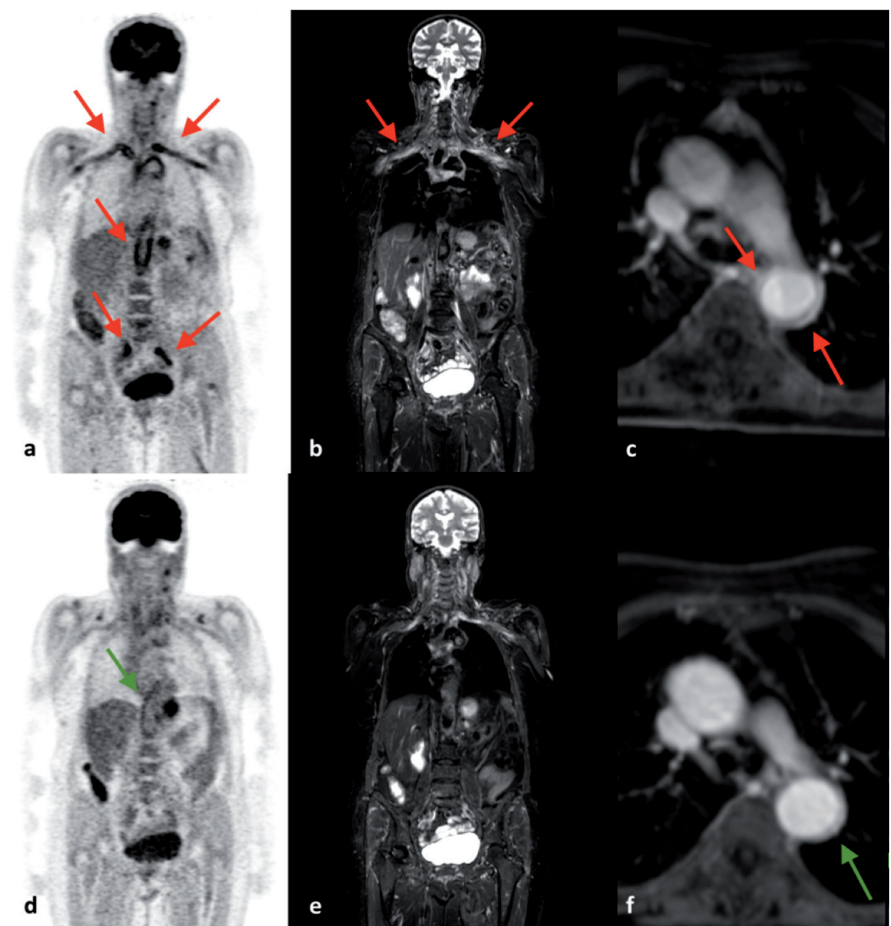


**Fig. 1.** At the first visit, coronal PET (a), coronal T2 STIR (b), and axial T1 VIBE (c) show extensive large-vessel vasculitis with aortitis and inflammatory affection of the supraortic branches and iliac arteries in a 63-year-old patient with giant cell aortitis (inflammatory lesions are marked by red arrows). After immunosuppressive treatment, PET and MRI demonstrate regressive inflammatory changes at the second visit (23 months later), with completely disappearing oedema at the subclavian arteries (e) and only low levels of residual disease activity at the aorta, as shown on PET and T1 VIBE (d, f; green arrows). CRP was normal and ESR was slightly elevated (*i.e.* 34 mm/h) and signs of clinical disease activity were absent at the second visit.

the first 2 visits, as described above). Moreover, in 1 patient with LVV, disease relapse was revealed by PET and MRI in 1 study at the level of the descending thoracic aorta, accompanied by a significantly growing aneurysm with partial thrombosis.

*Clinical and laboratory data*

Clinical assessment suggested active disease in 10/12 (83.3%) and 5/12 (41.7%) patients at the first and second visit ( $p=0.063$ ), respectively. At the third and fourth visit, 2/6 (33.3%) patients showed findings suggestive of clinically active disease in 3/10 (30%) studies. CRP and/or ESR were elevated in 10/12 (83.3%) patients at the first visit and 6/12 (50%) patients at the second visit. Additionally, absolute CRP and ESR values were significantly lower at the second visit compared to the first visit (Table II). A clinically relevant decrease (*i.e.* normalisation) was observed at the second visit in 6/12 (50%) and 4/12 (33.3%) patients for CRP and ESR, respectively. Increased inflammatory markers were observed in 1 patient during the third visit.

*PET/MRI versus clinical and laboratory data*

PET/MRI suggested active A/CPA in 22/34 (64.7%) studies, comprising 20 positive PET studies and 21 positive MRI studies. However, clinical assessment revealed positive findings at only 18/34 (52.9%) visits, and serological analysis showed elevated values at 17/34 (50%) visits (Table III). Disease status findings thus differed between methods: in comparison to PET/MRI, clinical assessment and serological analysis showed discordant findings at 8/34 (23.5%; *i.e.* 6 negative and 2 positive cases *versus* 6 positive and 2 negative PET/MRI studies) and 9/34 (26.5%; *i.e.* 7 negative and 2 positive cases *versus* 7 positive and 2 negative PET/MRI studies) visits, respectively. Two patients with negative serological findings and positive PET/MRI studies did not receive previous therapy at first visit. Moreover, relative changes in PET/MRI parameters and laboratory data between the first and second visit were not correlated significantly (Table IV).

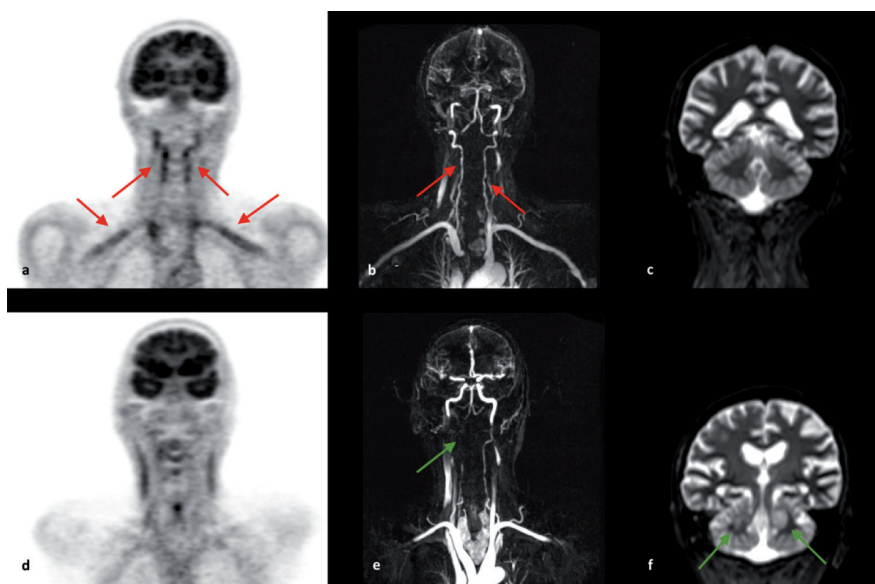


**Fig. 2.** In a 71-year-old patient with giant cell aortitis, coronal PET shows inflammatory involvement of both vertebral arteries and subclavian arteries (a). CE-MRA demonstrates multiple segmental stenoses in both vertebral arteries, whereas the subclavian arteries show no findings suggestive of vasculitis (b). During immunosuppressive treatment, vascular activity, as shown by PET, had disappeared at the second visit 4 months later (d). However, CE-MRA demonstrates a new, long segmental occlusion of the right vertebral artery (e, green arrow), resulting in new focal ischaemic lesions of the cerebellum, as indicated by T2 STIR (f vs. c, green arrows). Clinical symptoms were suggestive for stroke. CrP and ESR were both elevated at the first and second visit.



**Fig. 3.** Coronal maximum-intensity projection PET images of a 58-year-old patient with IRF, taken at different time points during the course of immunosuppressive treatment. At the first visit, PET shows typical active IRF (red arrows) with consecutive left-sided hydronephrosis (white arrow). At the second visit (2 months later), inflammatory activity has significantly decreased during immunosuppressive treatment. However, after finishing immunosuppressive therapy, PET/MRI shows disease relapse 17 months later at the third visit (red arrow), hydronephrosis on both sides (white arrows), and new onset of thoracic and supraaortic LVV (green arrows). After restarting immunosuppressive treatment, vascular/perivascular inflammation substantially decreased with only low levels of residual activity, but hydronephrosis remained and even worsened bilaterally (white arrows) at the fourth visit.

**Discussion**

This study investigated the value of fully integrated whole-body <sup>18</sup>F-FDG PET/MRI for monitoring disease ac-

tivity in patients with A/CPA during immunosuppressive therapy, in comparison to that of established clinical and serological markers; this has not

**Table III.** Number of patients with active A/CPA according to PET/MRI analysis and results of clinical and serological assessment at baseline (1st visit) and follow-up (2<sup>nd</sup> to 4<sup>th</sup> visit).

	1 <sup>st</sup> Visit (n*=12)	2 <sup>nd</sup> Visit (n*=12)	3 <sup>rd</sup> Visit (n*=6)	4 <sup>th</sup> Visit (n*=4)
PET/MRI**	12	5	3	2
Clinical assessment**	10	5	2	1
Serological assessment**	10	6	1	0

\*number of visits. \*\*number of patients with active A/CPA.

**Table IV.** Spearman’s rank correlation coefficient between the relative changes in imaging and laboratory markers (only metric values were used for statistical analysis).

	SUVmax	TBR	mPETVAS	MT
CrP	-0.029 (p=0.840)	0.291 (p=0.354)	-0.110 (p=0.610)	-0.411 (p=0.614)
ESR	-0.069 (p=0.832)	0.365 (p=0.242)	0.4171 (p=0.177)	-0.117 (p=0.561)

ESR: erythrocyte sedimentation rate.

been reported previously. Our assessments of disease activity status differed between PET/MRI, and clinical assessment and serological analysis, in approximately 25% of all visits. Moreover, relative changes between repeated visits in PET/MRI parameters and serologic markers did not correlate with each other. Thus, PET/MRI provides data on vascular/perivascular inflammation that is complementary to, and unique from clinical and laboratory assessments; this highlights the potential value of imaging-based disease activity monitoring, which might have a crucial impact on further clinical management in patients with A/CPA.

In clinical routine, A/CPA activity is usually assessed by means of clinical examination and acute-phase reactants, such as CRP and ESR. However, A/CPA clinical features may be non-specific and CRP and ESR can only be used with caution (6, 9, 12, 30, 31), as also illustrated by our study results, showing discordant laboratory parameter findings at 9 visits, as compared to PET/MRI, respectively. Furthermore, we did not observe statistically significant correlations of relative parameter changes between PET/MRI and acute-phase reactants during immunosuppressive therapy, suggesting an additional role for molecular hybrid-imaging for monitoring disease activity. Moreover, clinical

assessment indicated negative results at 6 visits and positive results at 2 visits, which was contrary to the findings of PET/MRI. Hence, laboratory and clinical markers may be substantially compromised during immunosuppressive therapy, suggesting the need for regular imaging follow-up to detect persistent inflammation. Of note, in 2 of 7 patients without previous therapy at baseline, inflammatory parameters were in the normal range, despite strong inflammation indications on PET/MRI, suggesting that the discrepancy between inflammatory parameters and the presence of inflammatory activity as assessed by PET/MRI may exist independently of previous immunosuppressive therapy.

While previous imaging studies for monitoring of A/CPA have focused on PET/CT, perfusion-based CT, and MRI (8, 13, 21, 32, 33), our study was the first to have investigated fully integrated PET/MRI as a one-stop multimodality approach to objectify changes in disease activity in patients with A/CPA under immunosuppressive therapy. Since qualitative and quantitative PET and MRI parameters yield unique and complementary data, the combination of this valuable information into a single examination may offer several benefits for diagnosis and patient comfort. To date, a few studies have reported comparable diagnostic performance of

PET and MRI with respect to disease activity in patients with LVV and retroperitoneal fibrosis, respectively (6, 21, 34, 35). This agreed with our study findings, which showed discrepant PET and MRI results in only 2 patients. Next, in agreement with other reports (18, 21, 22), our data showed substantial improvement of various potential inflammatory biomarkers (*i.e.* SUV<sub>max</sub>, TBR, 4-point VS, PETVAS, aortic/periaortic wall-thickening, enhancement, and oedema) under immunosuppressive therapy with comparable results of PET and MRI. Of note, PET parameters (VS) and MRI parameters (ICE and T2w-imaging) showed a clinically relevant (*i.e.* normalisation) decrease in more patients than did clinical and laboratory markers, indicating their potentially superior role in assessing response to treatment. However, aortic/periaortic wall-thickening never completely normalised during therapy, leading to the diagnostic dilemma of differentiating residual disease activity from burned-out/fibrotic lesions. Thus, complementary MRI data, such as contrast-enhanced and T2w-images as well as molecular PET data are essential for assessing the level of disease activity with high confidence. Indeed, contrast-enhanced MRI and T2w-imaging showed similar performance during the course of therapy, indicating the potential value of native oedema imaging as a proxy for active inflammation. Given the growing discussion about side-effects and deposits of Gadolinium-based contrast media application (36), a broader use of T2w MRI should be considered in inflammatory disorders with vascular involvement. Additionally, diffusion-weighted imaging might be an interesting alternative or complementary approach for assessing the activity of A/CPA (21, 35, 37). Nevertheless, contrast media application may be particularly useful for studying the progression or non-progression of vascular damage, potentially leading to surgical intervention. In our study, CE-MRA demonstrated a new occlusion of the right vertebral artery, resulting in brain ischaemia, a new aortic ectasia, and a significantly growing, partially thrombosed aortic aneurysm in 3 patients.

Although our data show promising results for monitoring the course of A/CPA by multimodality and multiparametric imaging, the value of serial imaging for guiding treatment decisions remains controversial (38). Recently, new PET data have suggested a novel qualitative summary score, based on global arterial FDG uptake (*i.e.* PETVAS), which is of potential value for monitoring disease activity and even predicting clinical relapse in patients with LVV (22, 23). To date, PETVAS has not been used in CPA, since it is only assessing supradiaphragmatic arterial territories sparing typical CPA manifestations affecting the abdominal aorta and iliac arteries. In our study, a modified version of PETVAS containing more vascular territories to account for typical distribution patterns in A/CPA was able to monitor different levels of vascular/perivascular inflammation. Additionally, it may be useful for predicting progressive structural vessel damage, since the highest scores were observed in 2 of 3 patients with relevantly changing or new onset vessel alterations according to CE-MRA. Further prospective trials are warranted to determine the value of PETVAS and its modified version for monitoring disease activity in patients with A/CPA. The present preliminary study had some limitations. First, the study included only a limited number of patients due to the rarity of this disease. We did not perform statistical subgroup analysis comparing patients with aortitis *versus* patients with CPA, or intraindividual follow-up studies after the second visit, due to small sample size. Second, a contemporaneous histologic gold standard at each visit would have been preferable to determine if activity based on imaging and clinical/laboratory findings is truly indicative for active A/CPA, but was not feasible for practical and ethical reasons. Thus, it is unclear whether increased metabolic activity in PET and *e.g.* contrast enhancement and wall thickening in MRI, detected particularly in patients after/under immunosuppressive therapy, represent subclinical vasculitis (23), atherosclerosis (39), a secondary process such as vascular remodelling, hypoxia (40), or a com-

bination of these factors. Despite the lack of histologic confirmation, results from this study strongly suggest that positive PET/MRI findings are consistent with active vascular/perivascular inflammation since the methods used to define disease activity were consistent with general approaches employed in prior studies (6, 13, 23, 25, 41-46). Third, high-doses of glucocorticoids can hamper the diagnostic accuracy of PET and MRI in A/CPA (47, 48). Since the average glucocorticoid dose was modest at the timepoint of imaging, it is unlikely to have affected our results substantially.

In conclusion, our results encourage the use of fully integrated <sup>18</sup>F-FDG PET/MRI as a one-stop multimodality approach for monitoring disease activity of A/CPA under immunosuppressive therapy delivering complementary information to clinical and laboratory data. However, up to date it may be premature to monitor disease activity and base treatment decisions on imaging findings alone. Thus, standardised and validated imaging-based outcome measures of disease activity in A/CPA have to be defined by conducting complementary prospective studies. The Outcome Measures in Rheumatology (OMERACT) Vasculitis Working Group will establish outcome measures for use in clinical trials in patients with large-vessel vasculitis in the near future (49). Besides, potential benefits of advanced imaging approaches in A/CPA such as PET/MRI have to be balanced with potential risks, including radiation exposure and cost.

## References

1. RESTREPO CS, OCAZIOINEZ D, SURI R, VARGAS D: Aortitis: imaging spectrum of the infectious and inflammatory conditions of the aorta. *Radiographics* 2011; 31: 435-51.
2. VAGLIO A, SALVARANI C, BUZIO C: Retroperitoneal fibrosis. *Lancet* 2006; 367: 241-51.
3. PARUMS DV: The spectrum of chronic peri-aortitis. *Histopathology* 1990; 16: 423-31.
4. PALMISANO A, URBAN ML, CORRADI D *et al.*: Chronic periaortitis with thoracic aorta and epiaortic artery involvement: a systemic large vessel vasculitis? *Rheumatology* (Oxford) 2015; 54: 2004-9.
5. VAGLIO A, PIPITONE N, SALVARANI C: Chronic periaortitis: a large-vessel vasculitis? *Curr Opin Rheumatol* 2011; 23: 1-6.

6. THUERMEK K, EINSPIELER I, WOLFRAM S *et al.*: Disease activity and vascular involvement in retroperitoneal fibrosis: first experience with fully integrated <sup>18</sup>F-fluorodeoxyglucose positron emission tomography/magnetic resonance imaging compared to clinical and laboratory parameters. *Clin Exp Rheumatol* 2017; 35 (Suppl. 103): S146-54.
7. SALVARANI C, PIPITONE N, VERSARI A *et al.*: Positron emission tomography (PET): evaluation of chronic periaortitis. *Arthritis Rheum* 2005; 53: 298-303.
8. BIER G, KURUCAY M, HENES J *et al.*: Monitoring disease activity in patients with aortitis and chronic periaortitis undergoing immunosuppressive therapy by perfusion CT. *Acad Radiol* 2017; 24: 470-7.
9. BIER G, HENES J, EULENBRUCH C, XENITIDIS T, NIKOLAOU K, HORGER M: Perfusion-based assessment of disease activity in untreated and treated patients with aortitis and chronic periaortitis: correlation with CT morphological, clinical and serological data. *Br J Radiol* 2015; 88: 20150526.
10. BERGER CT, SOMMER G, ASCHWANDEN M, STAUB D, ROTTENBURGER C, DAIKELER T: The clinical benefit of imaging in the diagnosis and treatment of giant cell arteritis. *Swiss Med Wkly* 2018; 148: w14661.
11. SCHEEL PJ JR, FEELEY N: Retroperitoneal fibrosis: the clinical, laboratory, and radiographic presentation. *Medicine* (Baltimore) 2009; 88: 202-7.
12. HOFFMAN GS, AHMED AE: Surrogate markers of disease activity in patients with Takayasu arteritis. A preliminary report from The International Network for the Study of the Systemic Vasculitides (INSSYS). *Int J Cardiol* 1998; 66 (Suppl. 1): S191-4; discussion S5.
13. FERNANDO A, PATTISON J, HORSFIELD C, D'CRUZ D, COOK G, O'BRIEN T: [<sup>18</sup>F]-fluorodeoxyglucose positron emission tomography in the diagnosis, treatment stratification, and monitoring of patients with retroperitoneal fibrosis: a prospective clinical study. *Eur Urol* 2017; 71: 926-33.
14. LORICERA J, BLANCO R, CASTANEDA S *et al.*: Tocilizumab in refractory aortitis: study on 16 patients and literature review. *Clin Exp Rheumatol* 2014; 32 (Suppl. 82): S79-89.
15. BERGER CT, RECHER M, DAIKELER T: Interleukin-6 flags infection in tocilizumab-treated giant cell arteritis. *Rheumatology* 2018; 57: 196-7.
16. DIKES A, ASCHWANDEN M, IMFELD S *et al.*: Takayasu arteritis: active or not, that's the question. *Rheumatology* 2017; 56: 1818-9.
17. REICHENBACH S, ADLER S, BONEL H *et al.*: Magnetic resonance angiography in giant cell arteritis: results of a randomized controlled trial of tocilizumab in giant cell arteritis. *Rheumatology* 2018; 57: 982-6.
18. SPIRA D, XENITIDIS T, HENES J, HORGER M: MRI parametric monitoring of biological therapies in primary large vessel vasculitides: a pilot study. *Br J Radiol* 2016; 89: 20150892.
19. BRAUN J, BARALIAKOS X, FRUTH M: The role of <sup>18</sup>F-FDG positron emission tomography for the diagnosis of vasculitides. *Clin Exp Rheumatol* 2018; 36 (Suppl. 114): S108-14.
20. MONTI S, BOND M, FELICETTI M *et al.*:

- One year in review 2019: vasculitis. *Clin Exp Rheumatol* 2019; 37 (Suppl. 117): S3-19.
21. KAMPER L, DREGER NM, BRANDT AS *et al.*: Diffusion-weighted MRI and PET-CT in the follow up of chronic periaortitis. *Int J Cardiovasc Imaging* 2018; 34: 1779-85.
  22. BANERJEE S, QUINN KA, GRIBBONS KB *et al.*: Effect of treatment on imaging, clinical, and serologic assessments of disease activity in large-vessel vasculitis. *J Rheumatol* 2020; 47: 99-107.
  23. GRAYSON PC, ALEHASHEMI S, BAGHERI AA *et al.*: <sup>18</sup>F-fluorodeoxyglucose-positron emission tomography as an imaging biomarker in a prospective, longitudinal cohort of patients with large vessel vasculitis. *Arthritis Rheumatol* 2018; 70: 439-49.
  24. BLOCKMANS D, DE CEUNINCK L, VANDERSCHUEREN S, KNOCKAERT D, MORTELMANS L, BOBBAERS H: Repetitive <sup>18</sup>F-fluorodeoxyglucose positron emission tomography in giant cell arteritis: a prospective study of 35 patients. *Arthritis Rheum* 2006; 55: 131-7.
  25. DEJACO C, RAMIRO S, DUFTNER C *et al.*: EULAR recommendations for the use of imaging in large vessel vasculitis in clinical practice. *Ann Rheum Dis* 2018; 77: 636-43.
  26. EINSPIELER I, THURMEL K, PYKA T *et al.*: Imaging large vessel vasculitis with fully integrated PET/MRI: a pilot study. *Eur J Nucl Med Mol Imaging* 2015; 42: 1012-24.
  27. LAURENT C, RICARD L, FAIN O *et al.*: PET/MRI in large-vessel vasculitis: clinical value for diagnosis and assessment of disease activity. *Sci Rep* 2019; 9: 12388.
  28. DELSO G, FURST S, JAKOBY B *et al.*: Performance measurements of the Siemens mMR integrated whole-body PET/MR scanner. *J Nucl Med* 2011; 52: 1914-22.
  29. SLART RHJA, WRITING GROUP, REVIEWER GROUP *et al.*: FDG-PET/CT(A) imaging in large vessel vasculitis and polymyalgia rheumatica: joint procedural recommendation of the EANM, SNMMI, and the PET Interest Group (PIG), and endorsed by the ASNC. *Eur J Nucl Med Mol Imaging* 2018; 45: 1250-69.
  30. SALVARANI C, CANTINI F, BOIARDI L, HUNDER GG: Laboratory investigations useful in giant cell arteritis and Takayasu's arteritis. *Clin Exp Rheumatol* 2003; 21 (Suppl. 32): S23-8.
  31. MAGREY MN, HUSNI ME, KUSHNER I, CALABRESE LH: Do acute-phase reactants predict response to glucocorticoid therapy in retroperitoneal fibrosis? *Arthritis Rheum* 2009; 61: 674-9.
  32. BRULS S, COURTOIS A, NUSGENS B *et al.*: <sup>18</sup>F-FDG PET/CT in the Management of Aortitis. *Clin Nucl Med* 2016; 41: 28-33.
  33. MARTINEZ-RODRIGUEZ I, JIMENEZ-ALONSO M, QUIRCE R *et al.*: <sup>18</sup>F-FDG PET/CT in the follow-up of large-vessel vasculitis: A study of 37 consecutive patients. *Semin Arthritis Rheum* 2018; 47: 530-7.
  34. QUINN KA, AHLMAN MA, MALAYERI AA *et al.*: Comparison of magnetic resonance angiography and <sup>18</sup>F-fluorodeoxyglucose positron emission tomography in large-vessel vasculitis. *Ann Rheum Dis* 2018; 77: 1165-71.
  35. RUHLMANN V, POEPEL TD, BRANDT AS *et al.*: <sup>18</sup>F-FDG PET/MRI evaluation of retroperitoneal fibrosis: a simultaneous multiparametric approach for diagnosing active disease. *Eur J Nucl Med Mol Imaging* 2016; 43: 1646-52.
  36. ROGOSNITZKY M, BRANCH S: Gadolinium-based contrast agent toxicity: a review of known and proposed mechanisms. *Biometals* 2016; 29: 365-76.
  37. IRONI G, TOMBETTI E, NAPOLITANO A *et al.*: Diffusion-weighted magnetic resonance imaging detects vessel wall inflammation in patients with giant cell arteritis. *JACC Cardiovasc Imaging* 2018; 11: 1879-82.
  38. DUFTNER C, DEJACO C, SEPRIANO A, FALZON L, SCHMIDT WA, RAMIRO S: Imaging in diagnosis, outcome prediction and monitoring of large vessel vasculitis: a systematic literature review and meta-analysis informing the EULAR recommendations. *RMD Open* 2018; 4: e000612.
  39. HYAFIL F, VIGNE J: Imaging inflammation in atherosclerotic plaques: Just make it easy! *J Nucl Cardiol* 2019; 26: 1705-8.
  40. FOLCO EJ, SHEIKINE Y, ROCHA VZ *et al.*: Hypoxia but not inflammation augments glucose uptake in human macrophages: Implications for imaging atherosclerosis with <sup>18</sup>fluorine-labeled 2-deoxy-D-glucose positron emission tomography. *J Am Coll Cardiol* 2011; 58: 603-14.
  41. RAMAN SV, ANEJA A, JARJOUR WN: CMR in inflammatory vasculitis. *J Cardiovasc Magn Reson* 2012; 14: 82.
  42. BOTH M, AHMADI-SIMAB K, REUTER M *et al.*: MRI and FDG-PET in the assessment of inflammatory aortic arch syndrome in complicated courses of giant cell arteritis. *Ann Rheum Dis* 2008; 67: 1030-3.
  43. MELLER J, STRUTZ F, SIEFKER U *et al.*: Early diagnosis and follow-up of aortitis with [<sup>18</sup>F]FDG PET and MRI. *Eur J Nucl Med Mol Imaging* 2003; 30: 730-6.
  44. ANDREWS J, AL-NAHHAS A, PENNELL DJ *et al.*: Non-invasive imaging in the diagnosis and management of Takayasu's arteritis. *Ann Rheum Dis* 2004; 63: 995-1000.
  45. SOUSSAN M, NICOLAS P, SCHRAMM C *et al.*: Management of large-vessel vasculitis with FDG-PET: a systematic literature review and meta-analysis. *Medicine (Baltimore)* 2015; 94(14): e622.
  46. MURATORE F, PIPITONE N, SALVARANI C, SCHMIDT WA: Imaging of vasculitis: State of the art. *Best Pract Res Clin Rheumatol* 2016; 30: 688-706.
  47. NIELSEN BD, GORMSEN LC, HANSEN IT, KELLER KK, THERKILDSEN P, HAUGE EM: Three days of high-dose glucocorticoid treatment attenuates large-vessel <sup>18</sup>F-FDG uptake in large-vessel giant cell arteritis but with a limited impact on diagnostic accuracy. *Eur J Nucl Med Mol Imaging* 2018; 45: 1119-28.
  48. KLINK T, GEIGER J, BOTH M *et al.*: Giant cell arteritis: diagnostic accuracy of MR imaging of superficial cranial arteries in initial diagnosis-results from a multicenter trial. *Radiology* 2014; 273: 844-52.
  49. AYDIN SZ, ROBSON JC, SREIH AG *et al.*: Update on outcome measure development in large-vessel vasculitis: report from OMERACT 2018. *J Rheumatol* 2019; 46: 1198-201.